Development 140, 2280-2288 (2013) doi:10.1242/dev.096354

Scx$^+$/*Sox9*$^+$ progenitors contribute to the establishment of the junction between cartilage and tendon/ligament

Yuki Sugimoto[1], Aki Takimoto[1], Haruhiko Akiyama[2], Ralf Kist[3], Gerd Scherer[4], Takashi Nakamura[2], Yuji Hiraki[1] and Chisa Shukunami[1,*]

SUMMARY

SRY-box containing gene 9 (*Sox9*) and scleraxis (*Scx*) regulate cartilage and tendon formation, respectively. Here we report that murine *Scx*$^+$/*Sox9*$^+$ progenitors differentiate into chondrocytes and tenocytes/ligamentocytes to form the junction between cartilage and tendon/ligament. *Sox9* lineage tracing in the *Scx*$^+$ domain revealed that *Scx*$^+$ progenitors can be subdivided into two distinct populations with regard to their *Sox9* expression history: *Scx*$^+$/*Sox9*$^+$ and *Scx*$^+$/*Sox9*$^-$ progenitors. Tenocytes are derived from *Scx*$^+$/*Sox9*$^+$ and *Scx*$^+$/*Sox9*$^-$ progenitors. The closer the tendon is to the cartilaginous primordium, the more tenocytes arise from *Scx*$^+$/*Sox9*$^+$ progenitors. Ligamentocytes as well as the annulus fibrosus cells of the intervertebral discs are descendants of *Scx*$^+$/*Sox9*$^+$ progenitors. Conditional inactivation of *Sox9* in *Scx*$^+$/*Sox9*$^+$ cells causes defective formation in the attachment sites of tendons/ligaments into the cartilage, and in the annulus fibrosus of the intervertebral discs. Thus, the *Scx*$^+$/*Sox9*$^+$ progenitor pool is a unique multipotent cell population that gives rise to tenocytes, ligamentocytes and chondrocytes for the establishment of the chondro-tendinous/ligamentous junction.

KEY WORDS: Sox9, Scx, Tenocytes, Ligamentocytes, Chondrocytes, Mouse

INTRODUCTION

In vertebrates, coordinated body movement is ensured by a close functional and physical association of bones, muscles, tendons and ligaments. Tendons connect muscles to the skeletal components and function as force transmitters, whereas ligaments bind bones together to stabilize joints (Benjamin and Ralphs, 2000; Rumian et al., 2007). Cells in tendons and ligaments are categorized as special types of fibroblasts known as tenocytes and ligamentocytes (Benjamin and Ralphs, 2000). Unlike randomly distributed fibroblasts in loose connective tissues, tenocytes and ligamentocytes in dense connective tissues are highly organized and align in rows between parallel thick fibers, mainly consisting of type I collagen, that provide the major resistance to tensile forces (Amiel et al., 1984; Canty et al., 2004). By inserting dense regular type I collagen fibers into muscle from the myotendinous junction and into bone from the osteo-tendinous/ligamentous junction, which is termed the enthesis, tendons and ligaments integrate each musculoskeletal component into a single functional unit (Benjamin and Ralphs, 1998; Benjamin and Ralphs, 2000). To achieve this integration, progenitors for these cells need to be coordinately distributed at both sides of the junction, and then execute each differentiation program there. However, it is still unclear how the coordinated connection of the musculoskeletal components is established by tendon/ligament progenitors during development.

Progenitors for tendons, ligaments, cartilage and bone arise from the sclerotome, the lateral plate mesoderm and the neural crest (Akiyama et al., 2005; Christ et al., 2004; Mori-Akiyama et al., 2003; Smith et al., 2005), whereas myogenic progenitors are derived from the myotome (Brent and Tabin, 2002). During the early stages of musculoskeletal development, these progenitor populations migrate and settle in the prospective region to give rise to cartilage, muscle, tendon and ligament primordia (Kardon, 1998). Each primordium for the musculoskeletal component initially develops as an individual unit, but subsequently they integrate with each other by an unknown mechanism.

Sox9, an SRY-related transcription factor that contains a high-mobility-group box DNA-binding domain, is an important regulator of cartilage formation. In *Sox9*-deficient chimeric embryos generated by the injection of *Sox9*$^{-/-}$ embryonic stem cells into *Sox9*$^{+/+}$ blastocysts, *Sox9*$^{-/-}$ cells are eliminated from cartilaginous primordia and are instead incorporated into the surrounding connective tissues (Bi et al., 1999). Conditional inactivation studies of *Sox9* using *Prx1Cre* or *Col2a1Cre* mice have revealed that *Sox9* is required for multiple steps of chondrogenic differentiation before and after cartilaginous condensation (Akiyama et al., 2002). In the tendon and ligament cell lineage, scleraxis (Scx), a basic helix-loop-helix transcription factor, is persistently expressed throughout differentiation (Pryce et al., 2007; Schweitzer et al., 2001). In *Scx*$^{-/-}$ mice, the intermuscular and force-transmitting tendons in the limbs and the tail tendons become hypoplastic, although the short appendicular anchoring tendons and ligaments are not significantly affected (Murchison et al., 2007). Such differential dependence on *Scx* expression suggests that tendons consist of distinct cell populations that have thus far not been defined.

At the early stages of musculoskeletal development, both *Sox9* and *Scx* are detected in the subpopulation of tendon/ligament progenitors and chondroprogenitors (Akiyama et al., 2005; Brent et al., 2005; Sugimoto et al., 2013). *Sox9* is upregulated during chondrogenesis (Zhao et al., 1997), whereas its expression is downregulated in association with the formation of the cruciate ligaments of the knee joint, the Achilles tendon and patella tendon (Soeda et al., 2010). *Scx* expression in the cartilaginous primordia is

[1]Department of Cellular Differentiation, Institute for Frontier Medical Sciences, Kyoto University, Kyoto 606-8507, Japan. [2]Department of Orthopaedics, Faculty of Medicine, Kyoto University, Kyoto 606-8507, Japan. [3]Centre for Oral Health Research, School of Dental Sciences, Newcastle University, Newcastle upon Tyne NE2 4BW, UK. [4]Institute of Human Genetics, Faculty of Medicine, University of Freiburg, D-79104 Freiburg, Germany.

*Author for correspondence (shukunam@frontier.kyoto-u.ac.jp)

Accepted 27 March 2013

transient during chondrogenesis (Cserjesi et al., 1995; Sugimoto et al., 2013). Lineage analysis crossing *ScxCre* transgenic mice with reporter mice revealed that *Scx*$^+$ chondroprogenitors differentiate into chondrocytes near the chondro-tendinous/ligamentous junction (CTJ/CLJ) during mouse development (Sugimoto et al., 2013). These lines of evidence suggest that the expression of *Scx* and *Sox9* is coordinately regulated in the cell population bridging between cartilage and tendon/ligament. However, very little is known about the cellular origin or molecular mechanism that regulates the formation of the junction between cartilage and tendon/ligament.

Through detailed *Sox9* lineage tracing in *Scx*$^+$ cells, we found that the *Scx*$^+$ cell population can be divided into two distinct populations with or without their *Sox9* expression history, i.e. *Scx*$^+$/*Sox9*$^-$ and *Scx*$^+$/*Sox9*$^+$ progenitors. Tenocytes are derived from both *Scx*$^+$/*Sox9*$^-$ and *Scx*$^+$/*Sox9*$^+$ progenitors, whereas ligamentocytes arise from *Scx*$^+$/*Sox9*$^+$ progenitors. Chondrocytes around the CTJ/CLJ are descendants of *Scx*$^+$/*Sox9*$^+$ progenitors. The closer the tendon is to the cartilaginous primordium, the more tenocytes arise from *Scx*$^+$/*Sox9*$^+$ progenitors. Using loss-of-function approaches, we demonstrate that *Scx*$^+$/*Sox9*$^+$ progenitors functionally contribute to the establishment of the junction between hyaline cartilage and tendon/ligament.

MATERIALS AND METHODS

Animals and embryos

Mice were purchased from Japan SLC (Shizuoka, Japan) or from Shimizu Laboratory Supplies Co. (Kyoto, Japan). *ROSA26R* (*R26R*) (Soriano, 1999) or *Rosa-CAG-LSL-tdTomato* (*Ai14*) (Madisen et al., 2010) strains obtained from The Jackson Laboratory were crossed to generate the *Sox9*$^{Cre/+}$*;R26R* and *Sox9*$^{Cre/+}$*;Ai14* mice for *Sox9* lineage tracing. *Ai14* mice harbor a targeted mutation of the *Gt(ROSA)26Sor* locus with a *loxP*-flanked STOP cassette preventing transcription of a *CAG* promoter-driven red fluorescent protein variant, tdTomato. Generation of *ScxGFP* and *ScxCre* transgenic strains is reported elsewhere (Sugimoto et al., 2013). To generate *Sox9* conditional knockout mice, *Sox9-flox* (Kist et al., 2002) and *ScxCre* transgenic strains were crossed. All animal experimental procedures were approved by the Animal Care Committee of the Institute for Frontier Medical Sciences, Kyoto University and conformed to institutional guidelines for the study of vertebrates.

In situ hybridization

Antisense RNA probes were transcribed from linearized plasmids with a digoxigenin (DIG) RNA labeling kit (Roche) as previously described (Takimoto et al., 2009). For RNA probes, cDNAs for *Scx* and *Myog* were amplified by RT-PCR based on sequence information in GenBank (*Scx*, BC062161; *Myog*, BC068019). Mouse *Sox9* cDNA was described previously (Wagner et al., 1994). For frozen section *in situ* hybridization, mouse embryos were treated in 20% sucrose without any fixation and then embedded in Tissue-Tek OCT compound (Sakura Finetek) and sectioned at 8 µm. Frozen sections were postfixed with 4% paraformaldehyde in phosphate-buffered saline (PFA/PBS) for 10 minutes at room temperature and then carbethoxylated in PBS containing 0.1% diethylpyrocarbonate twice. Sections were treated in 5× SSC, and hybridization was performed at 58°C with DIG-labeled antisense RNA probes. Immunological detection of DIG-labeled RNA probes was with an anti-DIG antibody conjugated with alkaline phosphatase (anti-DIG-AP Fab fragment; Roche) and BM Purple (Roche).

Immunostaining

Embryos were fixed with 4% PFA/PBS at 4°C for 3 hours, immersed in a series of sucrose solutions (12%, 15% and 18% sucrose in PBS), frozen, and cryosectioned at 8 µm. For *Sox9*$^{Cre/+}$*;R26R* mice, specimens were treated with 20% sucrose at 4°C for 3 hours without prefixation, cryosectioned at 10 µm, and then fixed with ice-cold acetone. After washing with PBS, the slides were incubated with 2% skimmed milk in PBS for 20 minutes and incubated overnight at 4°C with primary antibodies diluted with 2% skimmed milk in PBS. After washing, the sections were incubated with goat anti-rat and anti-rabbit secondary antibodies conjugated to Alexa Fluor 488 or with goat anti-rabbit and anti-mouse secondary antibodies conjugated to Alexa Fluor 594 (Molecular Probes), and washed again in PBS. The primary antibodies used were anti-GFP (diluted 1:1000; Nakarai), anti-Sox9 (1:600; Chemicon), anti-tenomodulin (Tnmd) (1:1000) (Oshima et al., 2004; Shukunami et al., 2008), anti-chondromodulin 1 (Chm1) (1:1000; Cosmo Bio) and anti-type I collagen (1:500; Rockland). Nuclei were counterstained with 4′,6-diamidino-2-phenylindole (DAPI). The images were captured under a Leica DMRXA microscope equipped with a Leica DC500 camera.

Toluidine Blue and X-gal staining

For Toluidine Blue staining, deparaffinized and/or hydrated sections were stained with a 0.05% Toluidine Blue solution (pH 4) for 2-5 minutes as described (Takimoto et al., 2012). For X-gal staining, embryos were treated with 20% sucrose in PBS at 4°C, and embedded in Tissue-Tek OCT compound. Frozen sections were prepared at 14 µm. Before staining, the sections were treated with fixation solution (0.2% glutaraldehyde, 5 mM EGTA, 2 mM $MgCl_2$) at 4°C for 5 minutes. After washing (phosphate buffer containing 2 mM $MgCl_2$, 0.01% sodium deoxycholate, 0.02% Nonidet P40), the sections were incubated with X-gal staining solution (5 mM potassium ferrocyanide, 5 mM potassium ferricyanide, 1 mg/ml X-gal) at 37°C overnight.

Skeletal preparations

After fixation with 4% PFA/PBS, mouse embryos were dehydrated with ethanol. Skin and soft tissues were removed and the embryos were then stained with 0.015% Alcian Blue 8GX (Sigma). After clearing with 2% KOH, the embryos were stained with 0.05% Alizarin Red S (Wako) in 1% KOH and then cleared with 1% KOH.

RESULTS

The Scx$^+$ cell population in the axial and the appendicular mesenchyme contains two distinct subpopulations of progenitors

Scx is expressed in the tendogenic/ligamentogenic regions, as well as in the chondrogenic regions (Cserjesi et al., 1995; Sugimoto et al., 2013). *In situ* hybridization analysis revealed that *Scx*$^+$/*Sox9*$^+$ chondrogenic cells are predominantly distributed in and around the primordial enthesis between cartilage and tendon/ligament (supplementary material Fig. S1). To compare the expression domains of Sox9 in Scx$^+$ cells in more detail, we performed double immunostaining using antibodies against Sox9 and GFP in transgenic *ScxGFP* embryos that express enhanced green fluorescent protein (EGFP) under the control of the promoter and enhancer of mouse *Scx* (Fig. 1) (Sugimoto et al., 2013).

During axial musculoskeletal development, the paraxial mesoderm separates into the somites that eventually give rise to the vertebrae, ribs, tendons, ligaments, the dermis of the dorsal skin and muscles (Christ et al., 2004; Christ et al., 2000). In the thoracic somite at E10.5, Sox9 was expressed in the entire sclerotome, notochord and neural tube (Fig. 1A), whereas the dorsolateral sclerotome containing tendon progenitors was composed of Scx$^+$ cells (Fig. 1B). The dorsolateral sclerotome was positive for Sox9, but small numbers of Scx$^+$/Sox9$^+$ and Scx$^+$/Sox9$^-$ cells were observed in the dermomyotome (Fig. 1C). At E11.5, Scx$^+$/Sox9$^+$ cells were observed in the vertebral and rib primordia (supplementary material Fig. S2A,B), and Scx$^-$/Sox9$^+$ cells were surrounded by Scx$^+$/Sox9$^+$ and Scx$^+$/Sox9$^-$ cells (supplementary material Fig. S2C). At E13.5, Sox9 was detected in the cartilaginous primordia of the vertebral body, neural arch and ribs (Fig. 1D). By contrast, Scx was exclusively expressed in the vertebral and costal tendon primordia (Fig. 1E). As typically seen in the costal region, Sox9 and Scx exhibited non-overlapping expression patterns at this stage (Fig. 1F).

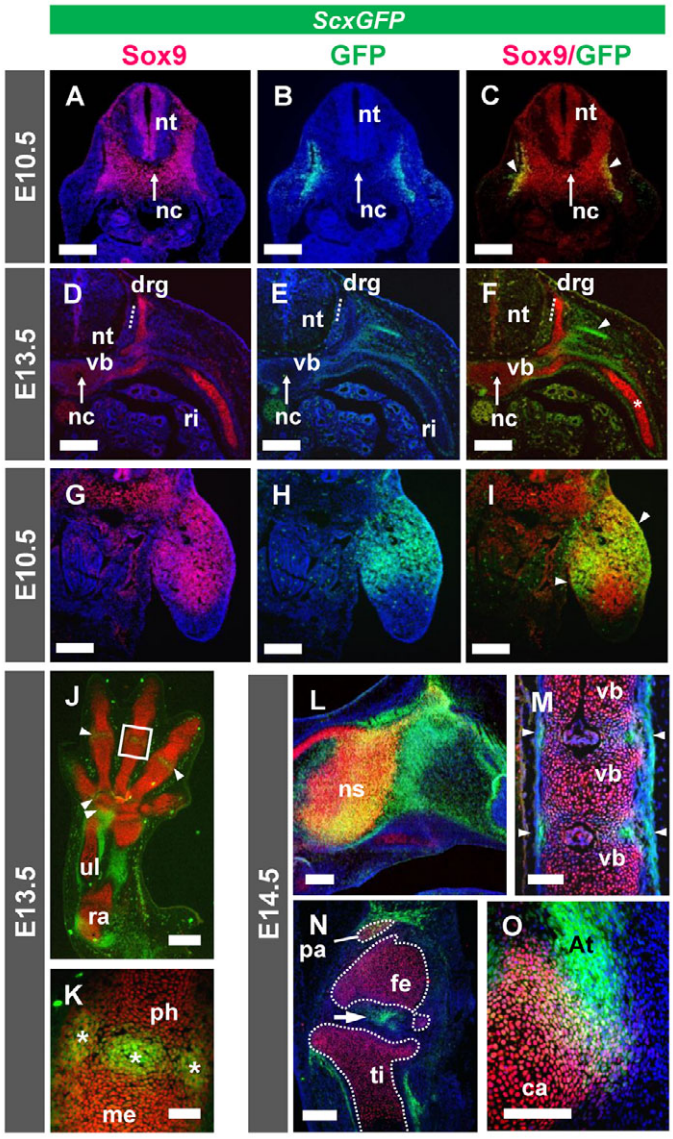

Fig. 1. Distribution of Sox9$^+$ and Sox9$^-$ cells in the Scx$^+$ region of mouse embryos. In *ScxGFP* transgenic mouse embryos, Sox9$^+$ cells (red) and Scx$^+$ cells expressing GFP (green) were detected by double immunostaining with antibodies specific for Sox9 and GFP, respectively, and nuclei were stained with DAPI (blue). Shown are transverse sections of the thoracic vertebrae at the forelimb level at E10.5 (**A-C**) and at the interlimb level at E13.5 (**D-F**); frontal sections of the forelimb at E10.5 (**G-I**); sagittal sections of the forelimb at E13.5 (**J**,**K**); and sagittal sections of the nasal region (**L**), vertebral column (**M**), the knee joint (**N**) and the heel (**O**) at E14.5. (C,F,I-O) Merged images are presented. The boxed region in J is magnified in K. An arrow in A-F indicates the notochord. Arrowheads in C indicate the dorsolateral sclerotome expressing both Sox9 and Scx. An arrowhead and an asterisk in F indicate a Scx$^+$ tendon and a Sox9$^+$ rib, respectively. The dotted line in D-F indicates the dorsal root ganglion. Arrowheads in I indicate a Scx$^+$/Sox9$^+$ region in the proximal part of the forelimb. Arrowheads in J and asterisks in K indicate Scx$^+$/Sox9$^+$ regions in the prospective joints of the forelimb. Arrowheads in M indicate Scx$^+$ intervertebral regions visualized by GFP expression. An arrow in N indicates the developing cruciate ligaments. Femur, tibia and patella are enclosed by the dotted lines. At, Achilles tendon; ca, calcaneus; drg, dorsal root ganglion; fe, femur; me, metacarpal; nc, notochord; ns, nasal septum; nt, neural tube; pa, patella; ph, phalanx; ra, radius; ri, rib; ti, tibia; ul, ulna; vb, vertebral body. Scale bars: 50 μm in K; 100 μm in O; 200 μm in A-C,G-I,L-N; 280 μm in D-F; 300 μm in J.

Appendicular and abdominal muscles are derived from the hypaxial myotome, whereas lateral plate mesoderm gives rise to the skeletal elements, tendons and ligaments of limbs (Brent and Tabin, 2002). At E10.5, overlapping expression of Sox9 and Scx was observed in the limb bud mesenchyme, except for the distal region (Fig. 1G-I). In the forelimb at E11.5, the primordia of the radius, ulna, carpal and metacarpal bone express *Sox9*. Scx$^+$/Sox9$^+$ or Scx$^+$/Sox9$^-$ cells then rearranged into the dorsal and ventral superficial regions surrounding the Sox9$^+$ region (supplementary material Fig. S2D-F). Scx$^+$/Sox9$^+$ cells were observed at the most proximal region of the limb (supplementary material Fig. S2F). At E13.5, the appendicular cartilaginous elements were positive for just Sox9 (Fig. 1J), but the collateral ligaments and the interzone of the metacarpophalangeal joint were double-positive for Sox9 and Scx (Fig. 1K). At E14.5, Scx$^+$/Sox9$^+$ and Scx$^+$/Sox9$^-$ cells were present in the cartilage of the nasal septum and the fibrous cells of the turbinate primordia, respectively (Fig. 1L). In the vertebral column, the outer layer of the intervertebral discs was Scx$^+$ (Fig. 1M). Scx$^+$/Sox9$^+$ chondrogenic cells were found in the entheseal region of the Achilles tendon and the patella (Fig. 1N,O).

Based on these data, we conclude that the Scx$^+$ cell population can be subdivided into two distinct subpopulations of Scx$^+$/Sox9$^+$ and Scx$^+$/Sox9$^-$ cells, and that *Sox9* expression later disappears from tendons and ligaments as differentiation proceeds.

The *Scx*$^+$/*Sox9*$^+$ progenitor pool gives rise to chondrocytes, tenocytes and ligamentocytes

For lineage tracing of *Sox9*$^+$ cells in the Scx$^+$ domains during tendon and ligament formation, we crossed *Sox9*$^{Cre/+}$ mice (Akiyama et al., 2005) with the reporter line *Rosa-CAG-LSL-tdTomato* (*Ai14*) (Madisen et al., 2010) to generate *Sox9*$^{Cre/+}$*;Ai14* mice, which were then crossed with *ScxGFP* mice to obtain *Sox9*$^{Cre/+}$*;Ai14;ScxGFP* embryos (Fig. 2A-E; Fig. 3A-G).

In *Sox9*$^{Cre/+}$*;Ai14;ScxGFP* embryos at E14.5, cells of the *Sox9*$^+$ lineage were found in the tendons near the vertebral column and ribs, joints between the ribs and vertebrae, and in the developing lung (Fig. 2A). The outer fibrous region of the vertebrae and the surrounding membranous regions consisted of *Scx*$^+$ cells that retained their *Sox9* expression history (Fig. 2B). In the tendinous diaphragm near the heart, most cells were negative for *Sox9* and positive for *Scx* (Fig. 2C). Abdominal tendons were positive for just *Scx* (Fig. 2D). In the tail, the insertion sites of the tendons into the vertebrae were derived from *Scx*$^+$/*Sox9*$^+$ progenitors, whereas tendons located further away from vertebrae were almost exclusively *Sox9*$^-$ and *Scx*$^+$ (Fig. 2E).

We then analyzed the contribution of *Sox9*$^+$ progenitors in the lumbar vertebrae and their associated tendons/ligaments of *Sox9*$^{Cre/+}$*;Ai14* neonates at the level of the vertebral body, the articular process or the spinous process (Fig. 2F-H; supplementary material Table S1). At P0, tendons and ligaments in the vicinity of vertebrae were derived from the *Sox9*$^+$ progenitor population (Fig. 2F-H). The lateral region of the thoracolumbar fascia enclosing the erector spinae muscles and tendons anchoring the latissimus dorsi muscle were negative for *Sox9* at P0 (Fig. 2H, T4, T3). Thus, *Scx*$^+$/*Sox9*$^+$ progenitors contribute to the formation of ligaments and tendons in the vicinity of ribs and vertebrae, whereas abdominal tendons are derived from the *Scx*$^+$/*Sox9*$^-$ cell lineage.

In the distal part of the hindlimb of *Sox9*$^{Cre/+}$*;Ai14;ScxGFP* embryos at E14.5, the ligaments arose from *Scx*$^+$/*Sox9*$^+$ progenitors, but both *Scx*$^+$/*Sox9*$^+$ and *Scx*$^+$/*Sox9*$^-$ progenitors contributed to tendon formation (Fig. 3A). *Scx*$^+$/*Sox9*$^+$ progenitors contributed to the formation of collateral ligaments (Fig. 3B, L3) and the entheseal

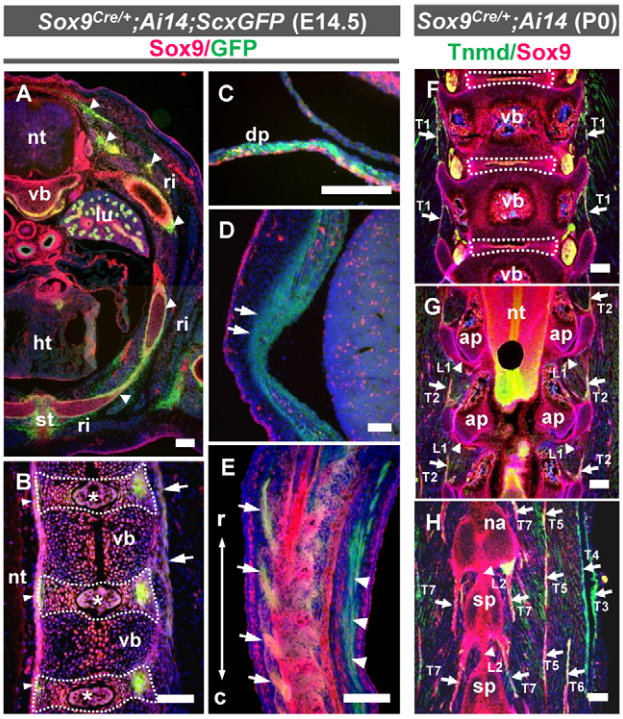

Fig. 2. Contribution of *Sox9*$^{+}$ progenitors to axial tendon and ligament formation. (**A-E**) Sections were prepared from *Sox9*$^{Cre/+}$*;Ai14;ScxGFP* embryos and cells of the *Sox9*$^{+}$ lineage were detected by tdTomato reporter expression and Scx^{+} cells were detected with anti-GFP antibody. (A) Transverse section of the trunk at the thoracic level. Arrowheads indicate the axial tendons associating with vertebrae and ribs. (B) A sagittal section of the vertebral column. The dotted lines enclose the developing intervertebral discs. Arrowheads, arrows and asterisks indicate the intervertebral annulus fibrosus, anterior longitudinal ligament and nucleus pulposus, respectively. (C) The diaphragm is shown in sagittal section. (D) A sagittal section of the abdomen, with arrows indicating the abdominal tendon in the body wall. (E) A sagittal section of the developing tail, with arrows and arrowheads indicating tendons associated and not associated with the vertebrae, respectively. Rostral and caudal sides are indicated by r and c, respectively. (**F-H**) Frontal sections of the vertebral column of *Sox9*$^{Cre/+}$*;Ai14* newborns at the vertebral bodies (F), the articular process (G) and the spinous process (H). *Sox9*$^{+}$ cells were detected via the expression pattern of tdTomato (red). Tnmd was visualized by immunostaining (green). Arrows in F-H and arrowheads in G,H indicate tendons and ligaments associated with the lumbar vertebral column, respectively. ap, articular process; dp, diaphragm; ht, heart; lu, lung; na, neural arch; nt, neural tube; ri, rib; sp, spinous process; st, sternum; vb, vertebral body. Scale bars: 200 µm.

side of tendons (Fig. 3C,D), whereas other parts of tendons mainly arose from *Scx*$^{+}$/*Sox9*$^{-}$ progenitors and the proportion of these cells varied between the individual tendons; for example, the extensor digitorum longus tendon was derived from *Scx*$^{+}$/*Sox9*$^{-}$ progenitors except for the prospective enthesis (Fig. 3B, T8), whereas Achilles tendons arose from both the *Scx*$^{+}$/*Sox9*$^{+}$ and *Scx*$^{+}$/*Sox9*$^{-}$ cell lineages (Fig. 3C,D, T9).

In the knee joint at E14.5, the primordia for cruciate and patella ligaments were visible as an *Scx*$^{+}$ region within the prospective joint cavity (Fig. 3E). All of the articular components and cartilage were positive for *Sox9* (Fig. 3F). The developing cruciate ligaments and capsular ligaments including the patella ligament and tibial collateral ligament were *Sox9*$^{+}$ (Fig. 3G). In the cruciate and the patella ligament at P0, Sox9 protein was no longer detectable in these tendons or ligaments, except for cartilage (Fig. 3H,I). Thus, all appendicular ligamentocytes arise from *Scx*$^{+}$/*Sox9*$^{+}$ progenitors, whereas appendicular tenocytes are derived from both the *Scx*$^{+}$/*Sox9*$^{+}$ and the *Scx*$^{+}$/*Sox9*$^{-}$ cell lineages.

Thus, the *Scx*$^{+}$/*Sox9*$^{+}$ progenitor pool is a unique multipotent cell population that gives rise to *Scx*$^{-}$/*Sox9*$^{+}$ chondrocytes and *Scx*$^{+}$/*Sox9*$^{-}$ tenocytes/ligamentocytes.

The closer the tendon is to the cartilaginous primordium, the more tenocytes arise from the *Sox9*$^{+}$ cell lineage

To investigate how *Sox9*$^{+}$ progenitors contribute to limb tendon formation, we analyzed the distribution of cells of the *Sox9*$^{+}$ lineage in Tnmd^{+} mature tendons and Chm1^{+} mature cartilage in the forearm of *Sox9*$^{Cre/+}$*;R26R* mice at P0 (Fig. 4A-L; supplementary material Table S1). Chm1 and Tnmd are markers of mature chondrocytes and tenocytes/ligamentocytes, respectively (Oshima et al., 2004; Shukunami et al., 2008; Shukunami et al., 2006).

Within the proximal parts of the ulna and radius, the sheet-like anchoring tendons consisted of tenocytes derived from *Sox9*$^{+}$ progenitors (Fig. 4A,G). By contrast, at the medial side of the ulna and radius, *Sox9*$^{+}$ progeny were absent from the proximal region of the cord-like force-transmitting tendons that were inserted into the individual muscles (Fig. 4B,H). However, tenocytes derived from *Sox9*$^{+}$ progenitors were found in the bundled force-transmitting tendons in the dorsal region of the distal ulna and radius and of the carpal levels (Fig. 4C,D,I,J). The forearm at the wrist level can be subdivided into several extensor tendon compartments with thick fascia. Within the same compartment, each tendon was derived from both *Sox9*$^{+}$ and *Sox9*$^{-}$ progenitors, and the ratio of *Sox9*$^{+}$ to *Sox9*$^{-}$ progenitor-derived tenocytes was similar (Fig. 4I,J). In carpal tendons, more of the tenocytes were derived from *Sox9*$^{+}$ progenitors (Fig. 4D,J). Tendons containing many *Sox9*$^{+}$ progenitor-derived tenocytes were inserted into the proximal edges of the metacarpals or carpals, whereas tendons containing fewer or no *Sox9*$^{+}$ progenitor-derived tenocytes were inserted into the middle or distal phalanges, in the more distal region of the autopod (Fig. 4D,J).

Around the metacarpal level, bundled tendons separate into individual tendons that insert into the end point of each digit (Fig. 4E,F). More tenocytes of the *Sox9*$^{+}$ cell lineage were observed in the tendons at the palmar side, including tendons of the flexor digitorium profundus (T26), flexor digitorium sublimis (T27) and interosseous (T30) (Fig. 4K,L), whereas most dorsal tendons (T18, T19) were *Sox9*$^{-}$ (Fig. 4E,K). In the collateral ligaments (L9) of the metacarpophalangeal joint, all ligamentocytes were strongly positive for *Sox9* (Fig. 4F,L). Although the force-transmitting tendons were derived from both *Sox9*$^{+}$ and *Sox9*$^{-}$ progenitors, the anchoring tendons near the elbow wholly arose from *Sox9*$^{+}$ progenitors (Fig. 4M).

Taken together, although the proportion of tenocytes that retain their *Sox9*$^{+}$ expression history varies between the individual force-transmitting tendons, in general the number of these *Sox9*$^{+}$ tenocytes decreases with increasing distance from the skeletal element.

Characterization of the transitional zone between cartilage and tendon/ligament

We then focused our analysis on the transitional zone between cartilage and tendon/ligament in order to reveal the contribution of *Sox9*$^{+}$ progenitors to the entheses. Entheses are classified into two

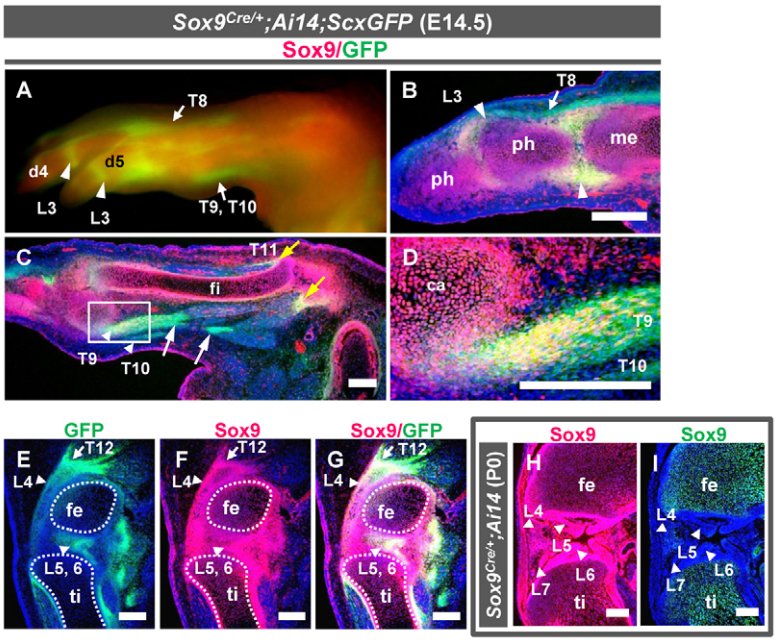

Fig. 3. Contribution of the *Scx*$^{+}$/*Sox9*$^{+}$ cell lineage to the formation of ligaments and the entheseal side of tendons. (**A-D**) Distribution of *Scx*-expressing tendons and ligaments (GFP, green) with a *Sox9* expression history (tdTomato, red) were analyzed in a *Sox9*$^{Cre/+}$*;Ai14;ScxGFP* mouse embryo at E14.5. Arrows and arrowheads indicate tendon and ligaments, respectively. (A) Lateral view of the hindlimb. (B-D) Sagittal sections of the hindlimb. The developing digit with the prospective digital joints is shown in B. White and yellow arrows in C indicate the force-transmitting and the anchoring tendons at the lower leg, respectively. The boxed region in C is shown at a higher magnification in D. (**E-I**) Sagittal sections of the knee joint prepared from *Sox9*$^{Cre/+}$*;Ai14;ScxGFP* embryos at E14.5 (E-G) or from *Sox9*$^{Cre/+}$*;Ai14* newborn mice (H,I). Developing cartilaginous primordia of the femur and tibia are enclosed by the dotted line. Scx^{+} cells (E,G, green) and Sox9^{+} cells (I, green) were detected by immunostaining with GFP and Sox9 antibodies, respectively. Cells derived from *Sox9*$^{+}$ progenitors were detected via expression of tdTomato (F-H, red). Arrowheads in E-I indicate ligaments of the knee joint. ca, calcaneus; d4, digit 4; d5, digit 5; fe, femur; fi, fibula; me, metacarpal; ph, phalanx; ti, tibia. Scale bars: 200 μm.

groups: fibrous and fibrocartilaginous (Benjamin and Ralphs, 2001). Collagen fibers in the fibrous entheses are inserted into bone via the periosteum, which gives a firmer hold to tendons and ligaments. Fibrocartilaginous entheses have four zones during the transition from tendon/ligament to bone, consisting of tendon/ligament, fibrocartilage, mineralized fibrocartilage, and bone. Fibrous entheses are mainly present in short ligaments or tendons. Since periosteum has been reported to be derived from *Sox9*$^{+}$ progenitors (Akiyama et al., 2005), we examined the prospective fibrocartilaginous entheses of quadriceps femoris tendon, cruciate ligaments and the Achilles tendon in *Sox9*$^{Cre/+}$*;R26R* mice (Fig. 5).

Type I collagen (Col1) and Chm1 were localized to tendons/ligaments including the prospective entheseal region and hyaline cartilage, respectively (Fig. 5A,D,G), whereas Tnmd was expressed in tendons and ligaments except for the region just adjacent to hyaline cartilage (Fig. 5B,E,H). These Col1^{+}/Tnmd^{-} cells were positive for X-gal staining (Fig. 5C,F,I). Hence, near the joint region, tenocytes, ligamentocytes and chondrocytes were derived from Sox9^{+} progenitors, but the prospective entheseal region abutting hyaline cartilage was negative for both Tnmd and Chm1, suggesting the presence of a distinct population in the prospective fibrocartilaginous enthesis bridging between hyaline cartilage and tendon/ligament.

Skeletal defects upon conditional inactivation of *Sox9* in *Scx*$^{+}$/*Sox9*$^{+}$ cells

We have generated two transgenic mouse lines that express *Cre* recombinase in the *Scx*$^{+}$ domains at high (*ScxCre-H*) or low (*ScxCre-L*) levels (Sugimoto et al., 2013). Owing to the expression gradient and transient expression of *Scx* around the entheseal cartilage (supplementary material Fig. S1), more chondrocytes in *ScxCre-H* are *Scx*$^{+}$ than in *ScxCre-L* (Sugimoto et al., 2013). To investigate the functional role of *Sox9* in *Scx*$^{+}$/*Sox9*$^{+}$ cells by a loss-of-function approach, we crossed these lines with *Sox9-flox* mice (Kist et al., 2002) to inactivate *Sox9* in *Scx*$^{+}$ cells. Both *ScxCre-L;Sox9*$^{flox/+}$ and *ScxCre-H;Sox9*$^{flox/+}$ mice were viable and fertile, but *ScxCre-L;Sox9*$^{flox/flox}$ and *ScxCre-H;Sox9*$^{flox/flox}$ mice died after birth. In *ScxCre-H;Sox9*$^{flox/flox}$ mice, severe skeletal hypoplasia was observed beyond the prospective entheseal cartilage, thus causing the secondary defects observed in tenocytes derived from *Scx*$^{+}$/*Sox9*$^{-}$ cells (not shown). Hence, we analyzed the *ScxCre-L;Sox9*$^{flox/flox}$ mice with skeletal defects around the entheseal cartilage in more detail.

In *ScxCre-L;Sox9*$^{flox/flox}$ neonates, the sternum and ribcage except for the proximal region were missing (Fig. 6A-D). In the vertebral column of *ScxCre-L;Sox9*$^{flox/flox}$ neonates, the vertebral bodies, the intervertebral discs, the articular processes of the neural arch and the transverse processes were hypoplastic (Fig. 6E,F). Severe hypoplasia in the ribcage is expected from the expression of *Scx* during the early stages of costal cartilage formation (Fig. 6M-O). The appendages of *ScxCre-L;Sox9*$^{flox/flox}$ mice were hypoplastic and shorter than those of controls and the joint cavity was smaller (Fig. 6A,B,G-L). In the forelimb of *ScxCre-L;Sox9*$^{flox/flox}$ mice, hypoplasia of carpal bones at the ulnar side, elbow joint, cartilage around the shoulder joint and deltoid tuberosity of the humerus was evident and curvature of the wrist was observed (Fig. 6G,H). Interestingly, abnormal mineralization occurred in the olecranon (Fig. 6G,H). In the hindlimb of *ScxCre-L;Sox9*$^{flox/flox}$ mice the tarsal bones, cartilage around the hip and the knee joint and tibial tuberosity were defective (Fig. 6I,J) and the patella was missing (Fig. 6K,L). These results suggest that skeletal dysplasia occurs in the *Scx*$^{+}$ cartilaginous region that is closely associated with tendons and ligaments.

Defective junction formation between cartilage and tendon/ligament upon conditional inactivation of *Sox9* in *Scx*$^{+}$/*Sox9*$^{+}$ cells

Double immunostaining of Tnmd and Chm1 revealed defective formation of the junction between cartilage and tendon/ligament in *ScxCre-L;Sox9*$^{flox/flox}$ at E18.5. Transverse processes of the lumber vertebrae (Fig. 7C) and the lateral region of sacral vertebrae (Fig. 7A) provide the attachment sites for axial tendons, but these sites were missing in *ScxCre-L;Sox9*$^{flox/flox}$ embryos (Fig. 7B,D). In control mice, Sox9^{+} cells were scattered in the outer annulus fibrosus near the inner annulus fibrosus (Fig. 7E), whereas these cells were missing in *ScxCre-L;Sox9*$^{flox/flox}$ embryos (Fig. 7F). In *ScxCre-L;Sox9*$^{flox/flox}$ intervertebral discs, the formation of the inner

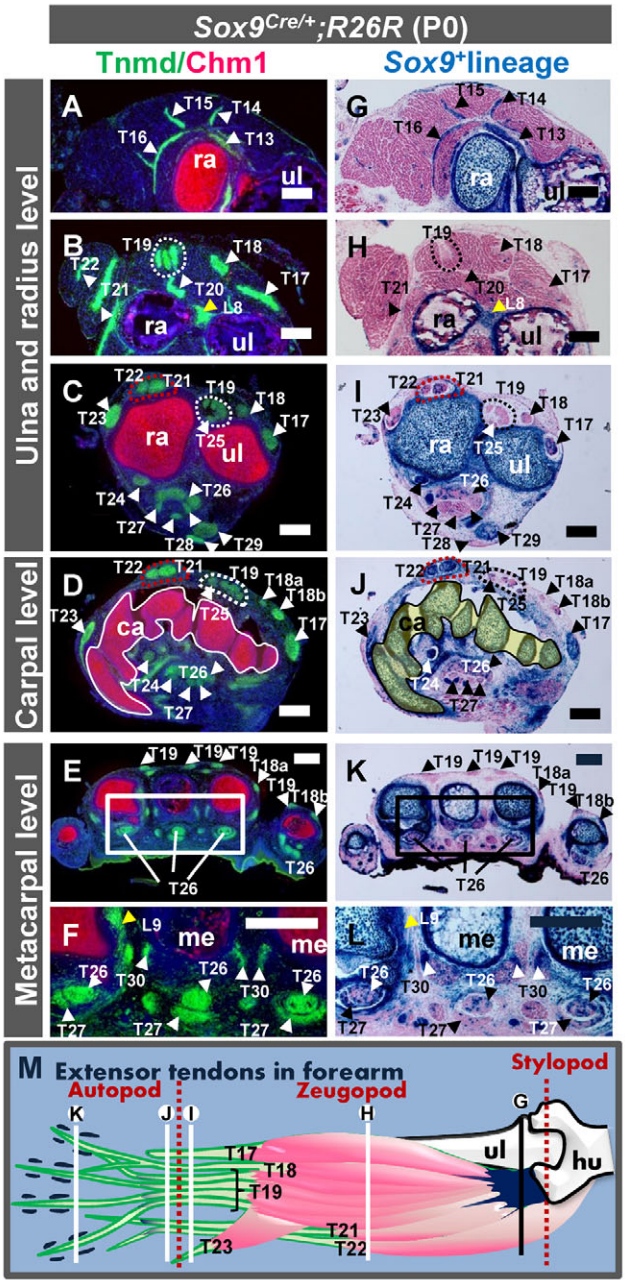

Fig. 4. Distribution of tenocytes derived from the *Sox9*$^{+}$ cell lineage in the forearm and digits. (**A-L**) Transverse sections of forearm prepared from *Sox9*$^{Cre/+}$*;R26R* neonates. Tnmd^{+} (green) and Chm1^{+} (red) regions were visualized by double immunostaining (A-F). Descendants of *Sox9*$^{+}$ progenitors were visualized by X-gal staining (G-L). Black or white arrowheads in A-L indicate tendons of the forearm. A yellow arrowhead in B,F,H,L indicates ligaments of the forearm. The boxed regions in E and K are shown at a higher magnification in F and L, respectively. The carpals are enclosed by a white or black solid line in D and J. The region enclosed by a red dotted line in C,D,I,J indicates tendons T21 and T22 (as defined in supplementary material Table S1). The region enclosed by a white or a black dotted line in B-D and H-J indicates tendons T19 and T25 (as defined in supplementary material Table S1). (**M**) Illustration of the distribution of tenocytes or ligamentocytes with a *Sox9*$^{+}$ lineage on the dorsal side of the mouse forearm. Bones (white), muscles (pink) and extensor tendons (light green) are shown. Dark blue indicates tenocytes and ligamentocytes with a *Sox9*$^{+}$ lineage. ca, carpal bones; hu, humerus; me, metacarpal; ra, radius; ul, ulna. Scale bars: 200 μm.

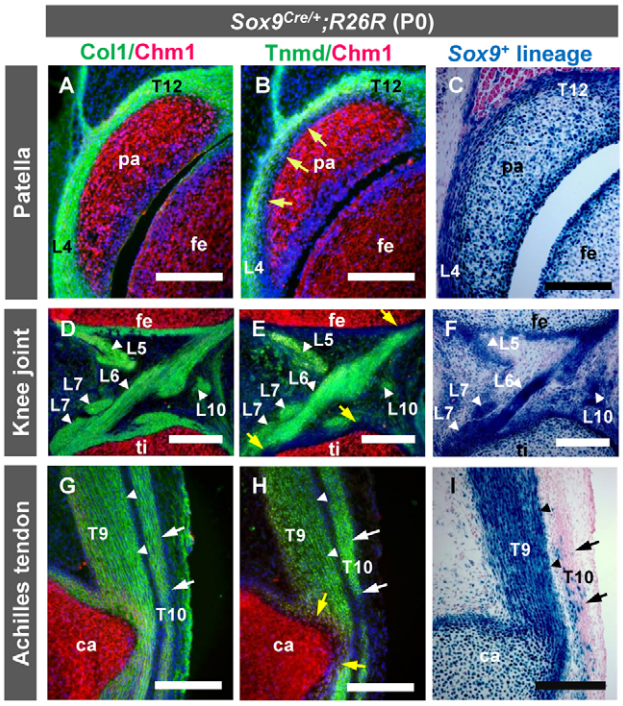

Fig. 5. Contribution of *Sox9*$^{+}$ progenitors to enthesis formation. Sagittal sections of the patella (**A-C**), the knee joint (**D-F**) and the Achilles tendon (**G-I**) from *Sox9*$^{Cre/+}$*;R26R* newborn mice. Col1^{+} (green in A,D,G), Tnmd^{+} (green in B,E,H) and Chm1^{+} (red in A,B,D,E,G,H) regions were visualized by double immunostaining. The distribution of X-gal-stained cells with a *Sox9*$^{+}$ lineage in the patella (C), the knee joint (F) and the Achilles tendon (I) is indicated. Arrowheads in D-F indicate ligaments in the knee joint. Arrowheads and arrows in G-I indicate the Achilles tendon (T9) and the superficial digital flexor tendon (T10), respectively. Yellow arrows indicate the Tnmd^{-}/Chm1^{-} region at the developing enthesis of the cruciate ligaments (L5 and L6 in E), the Achilles tendon (T9 in H) and the patella ligament (L4 in B). ca, calcaneus; fe, femur; pa, patella; ti, tibia; tl, talus. Scale bars: 200 μm.

annulus fibrosus, which shows metachromatic staining with Toluidine Blue, was defective, whereas the outer annulus fibrosus became wider (Fig. 7H) compared with that of control mice (Fig. 7G). Thus, in *ScxCre-L;Sox9*$^{flox/flox}$ embryos, the prospective entheses were either missing or hypoplastic in the axial skeleton.

In the forelimb, hypoplastic tendon formation in association with defective cartilage formation at the ulnar side was observed in *ScxCre-L;Sox9*$^{flox/flox}$ embryos at E16.5 (not shown). In the knee joint, the patella and the frontal region of the femoral condyle were missing (Fig. 7I,J). In the heel, the attachment site for the Achilles tendon was defective (Fig. 7K-N). Interestingly, cells just adjacent to the tendon attachment site, which are *Sox9*$^{+}$ in control mice, were missing in *ScxCre-L;Sox9*$^{flox/flox}$ embryos (Fig. 7O,P).

DISCUSSION

In this study, we have demonstrated for the first time that the *Scx*$^{+}$ cell population can be subdivided into two distinct populations with regard to their *Sox9* expression history: *Scx*$^{+}$/*Sox9*$^{+}$ and *Scx*$^{+}$/*Sox9*$^{-}$ progenitors. The *Scx*$^{+}$/*Sox9*$^{+}$ progenitor pool is a unique multipotent cell population that gives rise to *Scx*$^{-}$/*Sox9*$^{+}$ chondrocytes and *Scx*$^{+}$/*Sox9*$^{-}$ tenocytes/ligamentocytes (Fig. 8A). The closer the tendon and cartilage are to the prospective enthesis, the more tenocytes and chondrocytes originate from *Scx*$^{+}$/*Sox9*$^{+}$ progenitors (Fig. 8B).

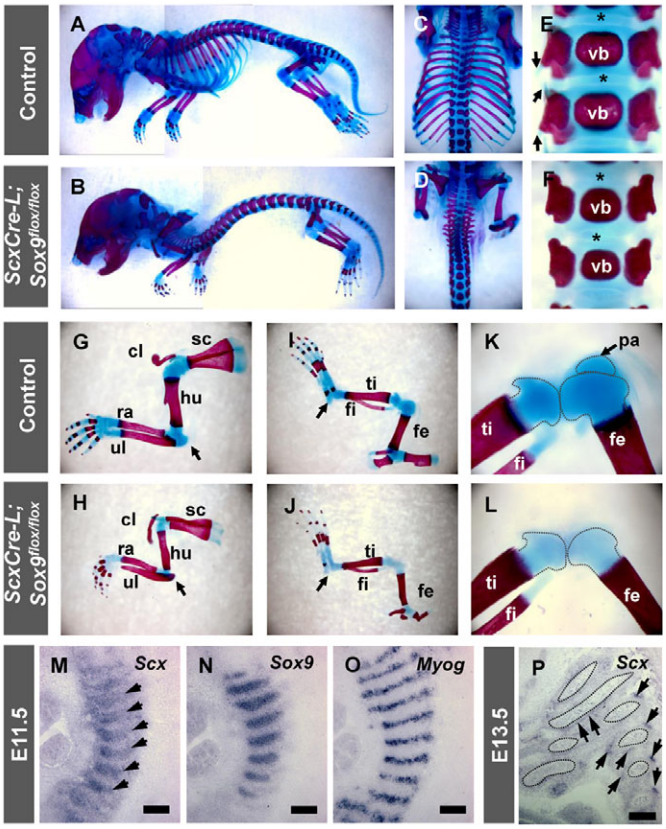

Fig. 6. Skeletal abnormalities upon loss of *Sox9* in *Scx*$^{+}$/*Sox9*$^{+}$ cells. (**A**,**B**) Lateral views of skeletal preparations of control (A) and *ScxCre-L;Sox9*$^{flox/flox}$ (B) mice at P0. (**C-F**) Dorsal views of the ribcage (C,D) and the vertebral bodies of the lumbar vertebrae (E,F) of control (C,E) and *ScxCre-L;Sox9*$^{flox/flox}$ (D,F) mice at P0. Arrows in E indicate the transverse process. Asterisks in E,F indicate the intervertebral discs of the lumbar vertebrae. (**G-L**) Appendicular skeletons of control (G,I,K) and *ScxCre-L;Sox9*$^{flox/flox}$ (H,J,L) mice at P0. Dorsal views of the forelimb (G,H) and lateral views of the hindlimb (I-L) are shown. The elbow joint (G,H), the calcaneous (I,J) and the patella (K) are indicated by an arrow. The dotted line in K,L encloses the epiphysis of the femur, the tibia and the patella. (**M-P**) *In situ* hybridization of *Scx* (M,P), *Sox9* (N) and *Myog* (O) on sagittal sections of the costal region of wild-type embryos at E11.5 (M-O) and E13.5 (P). *Scx* is detected in *Sox9*$^{+}$ rib primordia (arrows in M) and in the intercostal region including *Myog*$^{+}$ muscle primordia (O). Arrows in P indicate the *Scx*$^{+}$ costal tendons. Ribs are enclosed by the dotted lines. cl, clavicle; fe, femur; fi, fibula; hu, humerus; pa, patella; ra, radius; sc, scapula; ti, tibia; ul, ulna; vb, vertebral body. Scale bars: 200 μm.

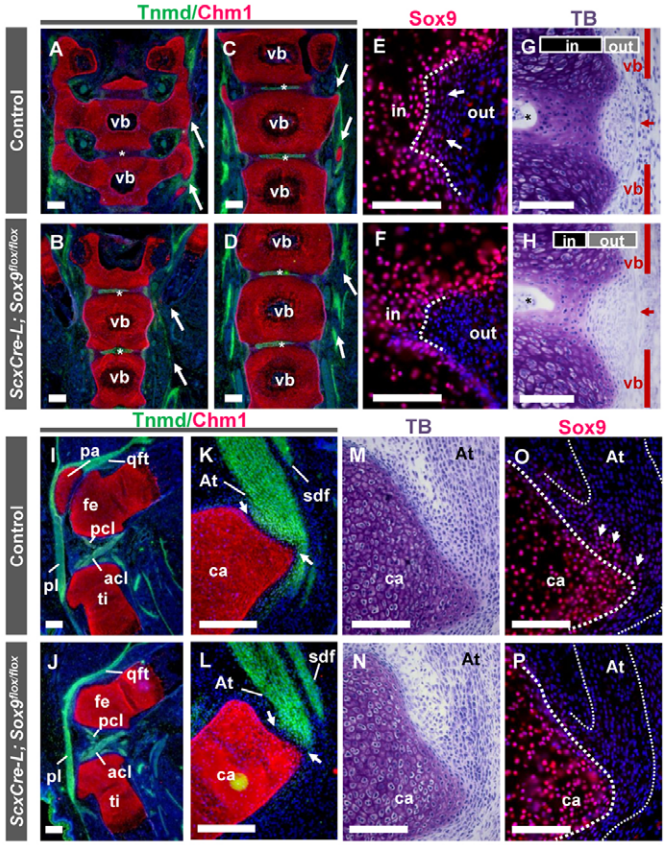

Fig. 7. Defective formation of the junction between cartilage and tendon/ligament upon loss of *Sox9* in *Scx*$^{+}$/*Sox9*$^{+}$ cells. (**A-F**) Frontal sections of the sacral (A,B) and lumbar (C-F) vertebrae of control (A,C,E) and *ScxCre-L;Sox9*$^{flox/flox}$ embryos (B,D,F) at E18.5. Tnmd^{+} (green) and Chm1^{+} (red) regions were visualized by double immunostaining (A-D). The lateral region (A) and the transverse processes (C) in the control are indicated by arrows, but those of *ScxCre-L;Sox9*$^{flox/flox}$ mice are missing (arrows in B,D). Asterisks in A-D indicate the nucleus pulposus of the intervertebral discs. Sox9^{+} cells are visualized by immunostaining (E,F). Arrows in E indicate Sox9^{+} cells in the outer annulus fibrosus of control mice. The dotted line in E,F encloses the outer annulus fibrosus. (**G**,**H**) Toluidine Blue staining of sagittal sections of the lumbar vertebrae of control (G) and *ScxCre-L;Sox9*$^{flox/flox}$ (H) mice at E18.5. Asterisks indicate the nucleus pulposus of the intervertebral disc. Black and gray boxes indicate the width of the inner (in) and outer (out) annulus fibrosus of the intervertebral disc. Red bars indicate the width of the vertebral body regions. An arrow indicates the intervertebral region. (**I-P**) Sagittal sections of the hindlimb of control (I,K,M,O) and *ScxCre-L;Sox9*$^{flox/flox}$ (J,L,N,P) mice at E18.5. Tnmd^{+} (green) and Chm1^{+} (red) regions were visualized by double immunostaining (I-L). The knee joint (I,J) and the attachment site of the Achilles tendon to the calcaneus (K,L) are shown. Arrows in K,L indicate the junction between hyaline cartilage and the Achilles tendon. Toluidine Blue staining (M,N) and the Sox9^{+} region visualized by immunostaining (red, O,P) are shown. The dotted line in O,P encloses the calcaneus and the Achilles tendon. Arrows in O indicate Sox9^{+} entheseal cells just adjacent to the hyaline cartilaginous calcaneus. acl, anterior cruciate ligament; At, Achilles tendon; ca, calcaneus; fe, femur; in, inner annulus fibrosus; out, outer annulus fibrosus; pa, patella; pcl, posterior cruciate ligament; pl, patella ligament; qft, quadriceps femoris tendon; vb, vertebral body; ti, tibia; sdf, superficial digital flexor tendon. Scale bars: 100 μm in E-H,M-P; 200 μm in A-D,I-L.

Further analyses of *ScxCre-L;Sox9*$^{flox/flox}$ mice revealed that the *Scx*$^{+}$/*Sox9*$^{+}$ cell population functionally contributes to the establishment of the junction between cartilage and tendon/ligament.

The *Scx*$^{+}$/*Sox9*$^{+}$ progenitor pool constitutes a multipotent cell population

Tenocytes are descendants of *Scx*$^{+}$/*Sox9*$^{+}$ and *Scx*$^{+}$/*Sox9*$^{-}$ progenitors (Fig. 8A). In general, the number of tenocytes that retain their *Sox9* expression history decreases with increasing distance from the skeletal element. Ligamentocytes and annulus fibrosus cells in the intervertebral discs are derived from *Scx*$^{+}$/*Sox9*$^{+}$ progenitors, whereas chondrocytes are derived from *Scx*$^{+}$/*Sox9*$^{+}$ and *Scx*$^{-}$/*Sox9*$^{+}$ progenitors (Fig. 8A). The closer the cartilage is to the prospective entheses, the more chondrocytes arise from *Scx*$^{+}$/*Sox9*$^{+}$ progenitors. Thus, the *Scx*$^{+}$/*Sox9*$^{+}$ progenitor population is predominantly distributed across the enthesis to form the CTJ/CLJ during development (Fig. 8B).

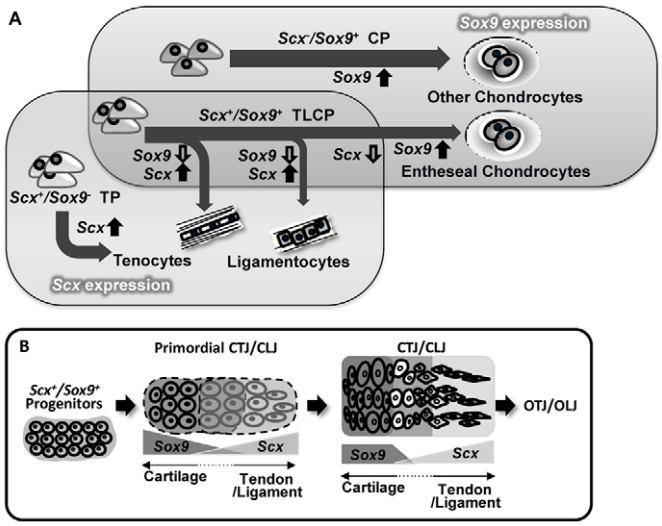

Fig. 8. Establishment of the junction between cartilage and tendon/ligament along the *Scx/Sox9* axis. (**A**) Differentiation of the tendogenic, ligamentogenic and chondrogenic cell lineages along the *Scx/Sox9* axis. The differentiation pathways of *Scx*$^{-}$/*Sox9*$^{+}$ chondroprogenitors (CP), *Scx*$^{+}$/*Sox9*$^{+}$ teno-/ligamento-/chondro-progenitors (TLCP) and *Scx*$^{+}$/*Sox9*$^{-}$ tenoprogenitors (TP) are shown. (**B**) Establishment of the chondro-tendinous/ligamentous junction (CTJ/CLJ) to form the osteo-tendinous/ligamentous junction (OTJ/OLJ). *Scx*$^{+}$/*Sox9*$^{+}$ progenitors give rise to the primordial CTJ/CLJ. The established CTJ/CLJ further develops to form the OTJ/OLJ during postnatal growth. Expression levels of *Sox9* and *Scx* are represented in dark and light gray, respectively.

In contrast to axial tendon formation, very little is known about axial ligament formation. We show that the *Scx*$^{+}$ axial ligaments are derived from the *Sox9*$^{+}$ cell lineage and thus conclude that these *Scx*$^{+}$ ligamentocytes originate from the *Sox9*$^{+}$ sclerotome. However, the timing of *Scx* expression in *Sox9*$^{+}$ ligament progenitors needs to be investigated further in order to clarify whether the axial ligament progenitors are derived from the *Scx*$^{+}$/*Sox9*$^{+}$ dorsolateral domain of the sclerotome or are recruited from the *Scx*$^{-}$ sclerotome to express *Scx* at later stages of development.

The appendicular tendons include a considerable number of tenocytes derived from *Scx*$^{+}$/*Sox9*$^{-}$ progenitors, particularly in the distal part of the limbs. Unlike the sclerotome, which consists of *Sox9*$^{+}$ progenitors, both *Sox9*$^{+}$ and *Sox9*$^{-}$ progenitors are present in the lateral plate mesoderm of the E10.5 limb bud. The *Scx*$^{+}$/*Sox9*$^{-}$ population in the lateral plate mesoderm might represent prospective distal tendon progenitors, although we cannot exclude the possibility that another, as yet unknown, population of tendon progenitors is recruited from the surrounding tissue to become *Scx*$^{+}$ tenocytes later in development.

Scx^{+}/*Sox9*$^{+}$ progenitors contribute to the establishment of the CTJ/CLJ

In *ScxCre-L;Sox9*$^{flox/flox}$ mice, the attachment sites of the tendons/ligaments to the cartilaginous primordia and the annulus fibrosus of the intervertebral discs are impaired. The most notable phenotype of *ScxCre-L;Sox9*$^{flox/flox}$ embryos is the absence of the ribcage. Chondrogenic cells in the developing costal cartilage have the ability to differentiate into entheseal chondrocytes, as evidenced by the expression of *Scx* in the entire rib cartilaginous primordium. This is compatible with the histological feature that costal chondrocytes are located very close to the tendinous attachment site of the surrounding intercostal muscle to each rib cartilage. Likewise, the cartilaginous bone primordium of the patella embedded in the tendon is missing. Thus, our loss-of-function analysis of *Sox9* in the *Scx*$^{+}$ domain reveals the functional significance of the *Scx*$^{+}$/*Sox9*$^{+}$ progenitor population in the establishment of the CTJ/CLJ, especially on the cartilaginous side.

In *Sox9*$^{flox/flox}$*;Prx1Cre* mice, inactivation of *Sox9* in limb bud mesenchyme causes the complete absence of cartilage and bone (Akiyama et al., 2002). Severe chondrodysplasia also occurs in *Sox9*$^{flox/flox}$*;Col2a1Cre* mice upon inactivation of *Sox9* in precartilaginous condensing cells and chondrocytes (Akiyama et al., 2002). Based on these findings, functional roles of *Sox9* in chondrogenesis could be discussed at three key stages: the chondroprogenitor stage, cartilaginous condensation stage and chondrocyte stage. Similarly, we consider tendo/ligamentogenesis in three distinct stages: the tendon/ligament progenitor stage, the tendon/ligament primordium formation stage, and tenocyte/ligamentocyte stage. In *ScxCre-L;Sox9*$^{flox/flox}$ embryos, we observed hypoplasia of the entheses of tendons/ligaments, the annulus fibrosus of the intervertebral discs, and of cartilages arising from *Scx*$^{+}$/*Sox9*$^{+}$ chondroprogenitors. The longer that *Sox9* expression continues, the more severe the defects within the *Scx*$^{+}$/*Sox9*$^{+}$ domain of *ScxCre-L;Sox9*$^{flox/flox}$ embryos become. Unlike chondrogenic cells, which continuously express *Sox9*, *Sox9* was downregulated in the migrating tendon/ligament progenitors before their arrival at the presumptive tendon/ligament-forming site. Considering the timing of *Sox9* downregulation in the tendon/ligament cell lineages, it is unlikely that the last two stages during tendo/ligamentogenesis critically depend on the function of *Sox9*. Loss of *Sox9* in *Scx*$^{+}$/*Sox9*$^{+}$ progenitors is likely to be a principal cause of the hypoplastic CTJ/CLJ in *ScxCre-L;Sox9*$^{flox/flox}$ mice.

Intervertebral discs and joints connect adjacent vertebrae. Each intervertebral disc is composed of an external annulus fibrosus surrounding an internal nucleus pulposus. Cells in the annulus fibrosus of intervertebral discs can be traced back to somitocoele cells that are included in the central core of the somite, distinct from the progenitor population for the vertebral body (Mittapalli et al., 2005). The annulus fibrosus consists of the inner annulus with chondrocytic cells and the outer annulus with tenocytic cells. We have shown here that both types of cells arise from *Scx*$^{+}$/*Sox9*$^{+}$ progenitors. In *ScxCre-L;Sox9*$^{flox/flox}$ mice, the inner annulus fibrosus is defective but expansion of the outer annulus fibrosus takes place on the ventral side. Thus, it is suggested that *Sox9* maintains the proper balance between the inner and the outer cell numbers by regulating the survival and differentiation of cells in the inner annulus fibrosus during intervertebral disc formation.

During postnatal growth, entheseal fibrocartilage develops in response to compressive loads (Benjamin and Ralphs, 1998). Fibrocartilage is an important connective structure between tendon and hyaline cartilage, but its cellular origin remains uncertain. We show that Chm1 and Tnmd are expressed in hyaline cartilage and tendon/ligament, respectively, whereas the transitional region just adjacent to hyaline cartilage or tendon/ligament is negative for Chm1 and Tnmd, consistent with our previous observation in rabbits (Yukata et al., 2010). Our lineage analysis further revealed that cells in this Tnmd^{-}/Chm1^{-} zone are positive for *Sox9* and *Scx*. Therefore, it is likely that cells in this transitional zone give rise to fibrochondrocytes during postnatal development. Further studies to reveal the cellular origin of fibrochondrocytes are now underway.

Acknowledgements
We thank Mr T. Matsushita and Ms K. Kogishi for histological studies and Ms H. Sugiyama for valuable secretarial help.

Funding
This study was partly supported by the Japan Society for the Promotion of Science (JSPS) [grants 22390289, 23659718].

Competing interests statement
The authors declare no competing financial interests.

Supplementary material
Supplementary material available online at
http://dev.biologists.org/lookup/suppl/doi:10.1242/dev.096354/-/DC1

References
Akiyama, H., Chaboissier, M. C., Martin, J. F., Schedl, A. and de Crombrugghe, B. (2002). The transcription factor Sox9 has essential roles in successive steps of the chondrocyte differentiation pathway and is required for expression of Sox5 and Sox6. *Genes Dev.* **16**, 2813-2828.
Akiyama, H., Kim, J. E., Nakashima, K., Balmes, G., Iwai, N., Deng, J. M., Zhang, Z., Martin, J. F., Behringer, R. R., Nakamura, T. et al. (2005). Osteo-chondroprogenitor cells are derived from Sox9 expressing precursors. *Proc. Natl. Acad. Sci. USA* **102**, 14665-14670.
Amiel, D., Frank, C., Harwood, F., Fronek, J. and Akeson, W. (1984). Tendons and ligaments: a morphological and biochemical comparison. *J. Orthop. Res.* **1**, 257-265.
Benjamin, M. and Ralphs, J. R. (1998). Fibrocartilage in tendons and ligaments – an adaptation to compressive load. *J. Anat.* **193**, 481-494.
Benjamin, M. and Ralphs, J. R. (2000). The cell and developmental biology of tendons and ligaments. *Int. Rev. Cytol.* **196**, 85-130.
Benjamin, M. and Ralphs, J. R. (2001). Entheses – the bony attachments of tendons and ligaments. *Ital. J. Anat. Embryol.* **106 Suppl. 1**, 151-157.
Bi, W., Deng, J. M., Zhang, Z., Behringer, R. R. and de Crombrugghe, B. (1999). Sox9 is required for cartilage formation. *Nat. Genet.* **22**, 85-89.
Brent, A. E. and Tabin, C. J. (2002). Developmental regulation of somite derivatives: muscle, cartilage and tendon. *Curr. Opin. Genet. Dev.* **12**, 548-557.
Brent, A. E., Braun, T. and Tabin, C. J. (2005). Genetic analysis of interactions between the somitic muscle, cartilage and tendon cell lineages during mouse development. *Development* **132**, 515-528.
Canty, E. G., Lu, Y., Meadows, R. S., Shaw, M. K., Holmes, D. F. and Kadler, K. E. (2004). Coalignment of plasma membrane channels and protrusions (fibripositors) specifies the parallelism of tendon. *J. Cell Biol.* **165**, 553-563.
Christ, B., Huang, R. and Wilting, J. (2000). The development of the avian vertebral column. *Anat. Embryol. (Berl.)* **202**, 179-194.
Christ, B., Huang, R. and Scaal, M. (2004). Formation and differentiation of the avian sclerotome. *Anat. Embryol. (Berl.)* **208**, 333-350.
Cserjesi, P., Brown, D., Ligon, K. L., Lyons, G. E., Copeland, N. G., Gilbert, D. J., Jenkins, N. A. and Olson, E. N. (1995). Scleraxis: a basic helix-loop-helix protein that prefigures skeletal formation during mouse embryogenesis. *Development* **121**, 1099-1110.
Kardon, G. (1998). Muscle and tendon morphogenesis in the avian hind limb. *Development* **125**, 4019-4032.
Kist, R., Schrewe, H., Balling, R. and Scherer, G. (2002). Conditional inactivation of Sox9: a mouse model for campomelic dysplasia. *Genesis* **32**, 121-123.
Madisen, L., Zwingman, T. A., Sunkin, S. M., Oh, S. W., Zariwala, H. A., Gu, H., Ng, L. L., Palmiter, R. D., Hawrylycz, M. J., Jones, A. R. et al. (2010). A robust and high-throughput Cre reporting and characterization system for the whole mouse brain. *Nat. Neurosci.* **13**, 133-140.
Mittapalli, V. R., Huang, R., Patel, K., Christ, B. and Scaal, M. (2005). Arthrotome: a specific joint forming compartment in the avian somite. *Dev. Dyn.* **234**, 48-53.
Mori-Akiyama, Y., Akiyama, H., Rowitch, D. H. and de Crombrugghe, B. (2003). Sox9 is required for determination of the chondrogenic cell lineage in the cranial neural crest. *Proc. Natl. Acad. Sci. USA* **100**, 9360-9365.
Murchison, N. D., Price, B. A., Conner, D. A., Keene, D. R., Olson, E. N., Tabin, C. J. and Schweitzer, R. (2007). Regulation of tendon differentiation by scleraxis distinguishes force-transmitting tendons from muscle-anchoring tendons. *Development* **134**, 2697-2708.
Oshima, Y., Sato, K., Tashiro, F., Miyazaki, J., Nishida, K., Hiraki, Y., Tano, Y. and Shukunami, C. (2004). Anti-angiogenic action of the C-terminal domain of tenomodulin that shares homology with chondromodulin-I. *J. Cell Sci.* **117**, 2731-2744.
Pryce, B. A., Brent, A. E., Murchison, N. D., Tabin, C. J. and Schweitzer, R. (2007). Generation of transgenic tendon reporters, ScxGFP and ScxAP, using regulatory elements of the scleraxis gene. *Dev. Dyn.* **236**, 1677-1682.
Rumian, A. P., Wallace, A. L. and Birch, H. L. (2007). Tendons and ligaments are anatomically distinct but overlap in molecular and morphological features – a comparative study in an ovine model. *J. Orthop. Res.* **25**, 458-464.
Schweitzer, R., Chyung, J. H., Murtaugh, L. C., Brent, A. E., Rosen, V., Olson, E. N., Lassar, A. and Tabin, C. J. (2001). Analysis of the tendon cell fate using Scleraxis, a specific marker for tendons and ligaments. *Development* **128**, 3855-3866.
Shukunami, C., Takimoto, A., Oro, M. and Hiraki, Y. (2006). Scleraxis positively regulates the expression of tenomodulin, a differentiation marker of tenocytes. *Dev. Biol.* **298**, 234-247.
Shukunami, C., Takimoto, A., Miura, S., Nishizaki, Y. and Hiraki, Y. (2008). Chondromodulin-I and tenomodulin are differentially expressed in the avascular mesenchyme during mouse and chick development. *Cell Tissue Res.* **332**, 111-122.
Smith, T. G., Sweetman, D., Patterson, M., Keyse, S. M. and Münsterberg, A. (2005). Feedback interactions between MKP3 and ERK MAP kinase control scleraxis expression and the specification of rib progenitors in the developing chick somite. *Development* **132**, 1305-1314.
Soeda, T., Deng, J. M., de Crombrugghe, B., Behringer, R. R., Nakamura, T. and Akiyama, H. (2010). Sox9-expressing precursors are the cellular origin of the cruciate ligament of the knee joint and the limb tendons. *Genesis* **48**, 635-644.
Soriano, P. (1999). Generalized lacZ expression with the ROSA26 Cre reporter strain. *Nat. Genet.* **21**, 70-71.
Sugimoto, Y., Takimoto, A., Hiraki, Y. and Shukunami, C. (2013). Generation and characterization of ScxCre transgenic mice. *Genesis* doi:10.1002/dvg.22372.
Takimoto, A., Nishizaki, Y., Hiraki, Y. and Shukunami, C. (2009). Differential actions of VEGF-A isoforms on perichondrial angiogenesis during endochondral bone formation. *Dev. Biol.* **332**, 196-211.
Takimoto, A., Oro, M., Hiraki, Y. and Shukunami, C. (2012). Direct conversion of tenocytes into chondrocytes by Sox9. *Exp. Cell Res.* **318**, 1492-1507.
Wagner, T., Wirth, J., Meyer, J., Zabel, B., Held, M., Zimmer, J., Pasantes, J., Bricarelli, F. D., Keutel, J., Hustert, E. et al. (1994). Autosomal sex reversal and campomelic dysplasia are caused by mutations in and around the SRY-related gene SOX9. *Cell* **79**, 1111-1120.
Yukata, K., Matsui, Y., Shukunami, C., Takimoto, A., Hirohashi, N., Ohtani, O., Kimura, T., Hiraki, Y. and Yasui, N. (2010). Differential expression of Tenomodulin and Chondromodulin-1 at the insertion site of the tendon reflects a phenotypic transition of the resident cells. *Tissue Cell* **42**, 116-120.
Zhao, Q., Eberspaecher, H., Lefebvre, V. and De Crombrugghe, B. (1997). Parallel expression of Sox9 and Col2a1 in cells undergoing chondrogenesis. *Dev. Dyn.* **209**, 377-386.